Initial stages of growth of the GaN(11$\bar{2}$2) layer on a nano-structured Si(113) substrate

© *V.N. Bessolov, E.V. Konenkova, S.N. Rodin*

Ioffe Institute,
194021 St. Petersburg, Russia
E-mail: lena@triat.mail.ioffe.ru

Scanning electron microscopy was used to study of the initial stages of the formation of a semipolar GaN(11$\bar{2}$2) layer during Metalorganic Chemical Vapor Deposition on Si(113) substrates, on the surface of which U-shaped grooves with element sizes < 100 nm (NP-Si(113)) were formed. It was found that NP-Si(113) substrates with a buffer AlN layer stimulate the formation of islands faceted by the planes m-GaN, c-GaN. It is shown that there is a predominant growth of the m-GaN facet in comparison with c-GaN. The experimental results correspond to the Gibbs–Curie–Wolff selection principle, but taking into account elastic stresses in the c-GaN plane.

Keywords: semipolar gallium nitride, nano-structured substrate, silicon.

1. Introduction

Optoelectronic devices using the polar plane GaN(0001) have a strong internal polarization field, which leads to spatial separation of electrons and holes in quantum wells and a decrease in the parameters of a number of devices (LEDs, lasers). One of the possible ways to increase the efficiency of quantum-dimensional structures based on gallium nitride is to grow structures in planes of nonpolar and semipolar orientations [1].

The use of Si as a structured substrate allows for synthesizing various orientations of GaN [2] crystals. However, the crystallographic mismatch of the lattices between GaN(0001) and Si(111) $\sim 17\%$ and the difference in thermal expansion coefficients (46%) create problems during the nucleation of the epitaxial layer and lead to deformation of the GaN/Si heterostructure [3]. The use of silicon as a substrate causes a number of additional difficulties, namely: the surface of Si is subject to oxidation, therefore, before the start of growth, it is necessary to remove the oxidized layer [4], at normal synthesis temperatures Ga reacts with Si, forming a eutectic alloy [5], which causes etching of silicon, called „backmelting" [6].

GaN epitaxy(11$\bar{2}$2) on microstructured substrates (113)Si by a combination of MOCVD (Metal Organic Chemical Vapor Deposition) and HVPE (Hydride Vapor Phase Epitaxy) methods was proposed by the authors of [7]. To suppress the effect of „backmelting" in the synthesis of semipolar (11$\bar{2}$2) GaN on a microstructured substrate Si(113) using the MOCVD method, a two-stage approach was applied in which, after the formation of the buffer layer AlN, one of the faces is covered with a layer of SiO$_2$ [8].

The initial stages of layer growth on a silicon substrate play an important role in the development of semi-polar and non-polar layers. The effect of crystal faceting of the buffer AlN layer on the structure of the semipolar GaN layer was demonstrated by Amano et al. [9]. The authors showed that it is possible using MOCVD method to synthesize various semipolar layers of GaN(10$\bar{1}$3) or GaN(10$\bar{1}$5) on Si(001) substrates if the magnetron sputtering method is used to pre-grow buffer layers of AlN, which have formed different inclination of the faces to the substrate surface. The use of faces of a structured substrate to control the structure of a semipolar layer was proposed by Nakamura et al. and it was named „epitaxy controlling the orientation" (orientation controlling epitaxy) [10].

Semipolar layers can be grown with upper surfaces having a GaN orientation (10$\bar{1}$1) [11] and GaN(11$\bar{2}$2) [8] depending on the technological conditions in case of synthesis of semipolar GaN layers on a structured Si(113) substrate.

This work covers the initial stages of growth of the GaN layer(11$\bar{2}$2) on a nanostructured Si(113) substrate, on the surface of which U-shaped grooves with element sizes < 100 nm are formed (Fig. 1).

The structural characteristics of the GaN layers were determined by X-ray diffraction analysis and scanning electron microscopy.

2. Experiment procedure

The substrates NP-Si(113) were formed using the technology described in [12]. The layers of buffer AlN and GaN layers were synthesized by the MOCVD method on a modified EpiQuip unit with a horizontal reactor similarly to [12]. Hydrogen was used as a carrier gas, and ammonia, trimethylgallium and trimethylaluminium as precursors. The structures consisted of an AlN layer with
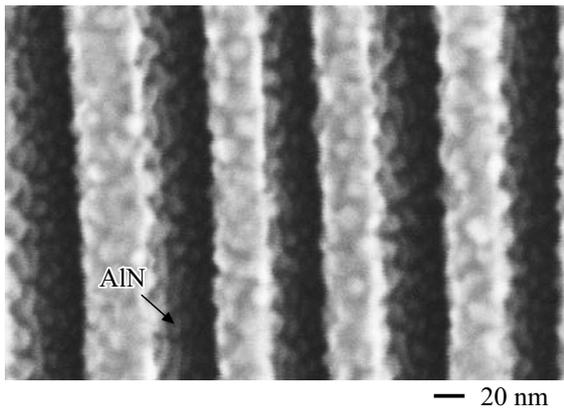
Figure 1. SEM is an image of the surface NP-Si(113) of a substrate coated with a thin layer AlN.

Specific surface energy in eV/A^2 of ideal AlN and GaN surfaces with polar, nonpolar and semipolar orientations [19]

	(0001)	(000$\bar{1}$)	(11$\bar{2}$2)	(11$\bar{2}$0)	(10$\bar{1}$0)
AlN	0.250	0.255	0.259	0.170	0.173
GaN	0.185	0.228	0.194	0.141	0.141

a thickness of ~ 20 nm and two types of GaN layers of different thickness: an insular GaN layer with dimensions of $\sim 0.05-0.1$ microns and a solid GaN layer (11$\bar{2}$2) with a thickness of $0.5-1$ microns. The insular layer was studied to clarify the picture of the initial stages of growth of the semipolar GaN-layer.

X-ray diffraction analysis of the layers showed that the solid layers of GaN(11$\bar{2}$2) have a half-width of the X-ray diffraction curve $\omega \sim 30$ arcmin. The surface morphology of semipolar GaN(10$\bar{1}$1) and GaN(11$\bar{2}$2) structures under epitaxy on nanostructured Si(100) and Si(113) substrates is given in [13], where it is shown that the formation of the GaN layer(11$\bar{2}$2) occurs from sufficiently large blocks.

3. Experimental results and discussion

The image of the surface in a scanning electron microscope showed that on an NP-Si(113) substrate, the AlN layer evenly covers the surface (Fig. 1), and GaN nucleation occurs on the AlN/Si(111) face by an island mechanism (Fig. 2), and the shape of the island (Fig. 3, a, b, c) shows the presence of faces „c-GaN", „m-GaN". The orientation of the islands in the array is set by the direction of the plane Si(111) of the nanochannels in NP-Si(113). The average thickness of the islands in the direction perpendicular to the groove was ~ 100 nm, (Fig. 3, a), and in the direction along the groove ~ 160 nm (Fig. 3, b). It can be seen that the crystals are cut both in the direction along the groove, in our opinion, — m-GaN with an angle $\sim 120°$ between the faces and C-GaN in a plane parallel to the face Si(111) (fig. 3, a, b, c). The face m-GaN has an edge that belongs to two adjacent planes m-GaN and lies parallel to the plane (11$\bar{2}$2). It can be seen that the selective growth of GaN(11$\bar{2}$2) on NP-Si(113) is accompanied by the formation of voids in the region of the bottom of the nanochannels, which provides stress relaxation in the GaN [14] layer and creates the perspective of separating thick layers using the Void Assisted Separation method (Fig. 2).

Note that the observed faceting of a GaN crystal during synthesis on a silicon substrate occurs as a result of nonequilibrium processes, which are influenced by the values of supersaturation of gallium atoms in a gaseous medium, crystal deformation during GaN/Si heteroepitaxy, as well as, possibly, the difference in the length of the diffusion path of Ga atoms in the directions along and across the groove. It has been experimentally shown that the formation of faces during epitaxial lateral overgrowth (ELOG) in GaN is controlled by a variety of growth parameters, such as temperature, pressure [15] and reagent flows [16].

As is known, the faces of GaN embryo should be formed in accordance with the Gibbs–Curie–Wolfe principles, which require the formation of a crystal with the lowest surface free energy. The facet of a crystal growing under equilibrium conditions is formed by facets with minimum values of specific surface energy [17]. Note that the components in crystals with covalent, ionic or metallic bonds strongly stick together upon collision, leaving them little room to adjust their position during crystallization, which makes it difficult to form the faces of [18]. Usually, when a crystal grows, its faces move in a direction perpendicular to their planes, and the higher the growth rate, the greater the specific surface energy of the face.

The authors of [15] calculated the specific surface energies of various GaN faces (see table). Although the calculations were carried out at 0 K, the general trends are also applicable at higher temperatures.

As can be seen from the table, the specific surface energy GaN(0001) of 0.185 eV/A^2 and GaN(10$\bar{1}$0) of
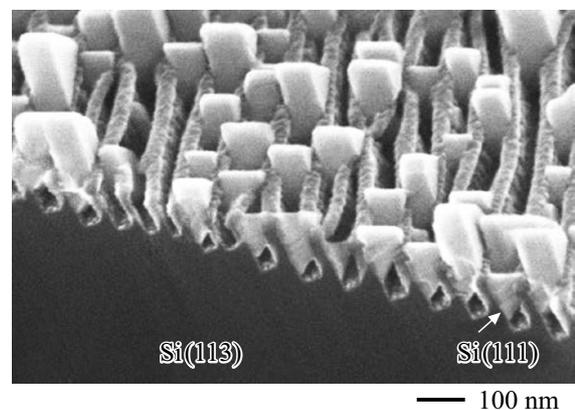
Figure 2. SEM is an image of the GaN insular layer at the initial stage of growth.
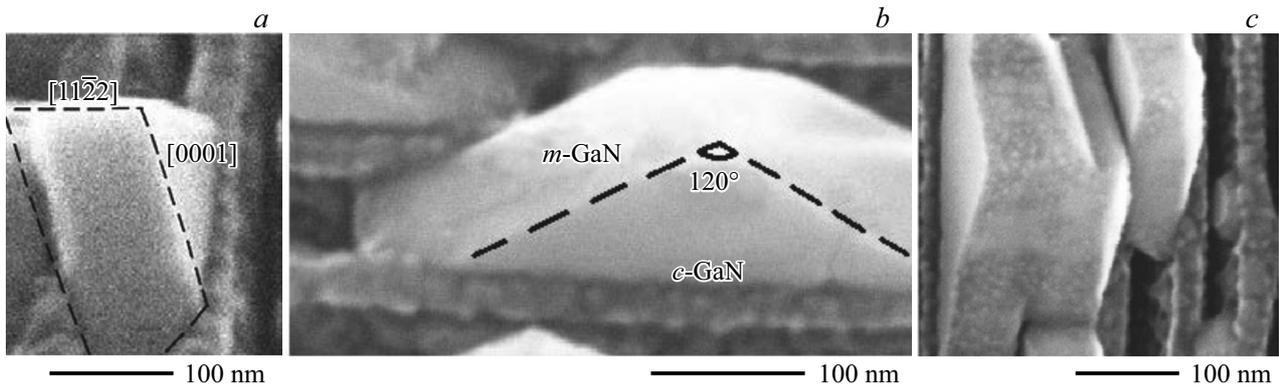
Figure 3. SAM-image of the faces of the island GaN: *a* — *m*-GaN, where the dotted lines represent the edges [11$\bar{2}$2] and [0001], *b* — *c*-GaN, *c* — top view of *m*-GaN and *c*-GaN.

0.141 eV/A^2 [19] imply that the growth rate of the *c*-GaN face should be greater than *m*-GaN, and consequently, the layer thickness in the direction of *c*-GaN should be greater than in the direction of *m*-GaN. However, this is not confirmed in the experiment. We believe that this behavior of the growth rate of the face *c*-GaN is due, perhaps, firstly, to the effect of the deformation of the face (0001) during epitaxy on the wall of the groove Si(111), which should reduce the value of the specific surface energy *c*-GaN, and secondly, the differences in the diffusion length of Ga atoms along and across the groove. The change in the value of the surface energy GaN(0001) under the impact of elastic stresses of the surface was noted in [20].

The appearance of the crystal configuration when the edge is parallel (11$\bar{2}$2) can be explained by the growth features of gas-phase epitaxy. All growth parameters can be represented by one thermodynamic epitaxy parameter — supersaturation of vapors Ga$-\gamma_{Ga}$, which measures the deviation of the system from equilibrium and represents the driving force for the formation of GaN and depends on the partial pressure Ga in the gas medium [21]

$$\gamma_{Ga} = \frac{\left(\left(P_{in}^{Ga}\right) - P_{ex}^{Ga}\right)}{P_{ex}^{Ga}},$$

where P_{in}^{Ga} is the input partial pressure, and P_{ex}^{Ga} is the equilibrium vapor pressure Ga at the interface of the vapor–solid body.

In turn, the chemical potential of gallium μ_{Ga} is associated with the oversaturation of Ga [21] atoms as

$$\mu_{Ga} \sim kT \log(1 + \gamma_{Ga}).$$

Calculations performed in [21] for three surfaces for μ_{Ga} showed that semipolar faces (11$\bar{2}$2) are formed at high supersaturation of Ga vapors, while nonpolar (11$\bar{2}$0) faces are preferable at low supersaturation of Ga vapors.

Such a different behavior of the nonpolar and semipolar faces of GaN is due to the peculiarities of the atomic bonds of the semipolar face. Semipolar surfaces were first defined by Baker et al. as planes passing diagonally through a
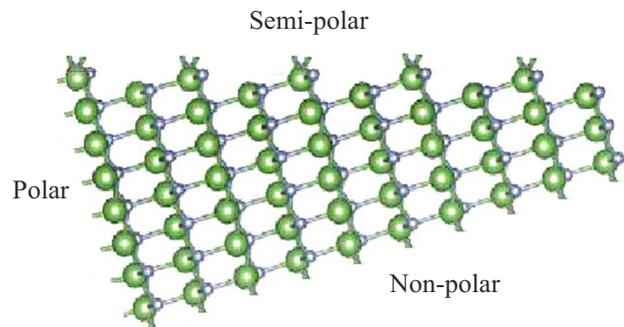
Figure 4. Cross-sectional model of polar, semi-polar and non-polar faces.

hexagonal elementary cell and forming a non-orthogonal angle with the *c*-plane [22] (Fig. 4).

An ideal semipolar face (11$\bar{2}$2) consists of rows of GaN dimers, each of which contains three broken bonds (one single, one double) in contrast to the polar or non-polar (11$\bar{2}$0), which consist of atoms having one broken bond (Fig. 4). The surface differences of the semipolar face from the polar and nonpolar ones lead both to a difference in the specific surface energy of the faces and to the crystallographic dependence of the face on the supersaturation of Ga atoms in the gas composition.

Just as with ELOG (Epitaxial Lateral Over Growth) epitaxy [23], in our experiments with a small value of γ_{Ga} and a higher value of the specific surface energy of the GaN face(11$\bar{2}$2), than for the GaN face(10$\bar{1}$0), there is an increase in the growth rate on the face (11$\bar{2}$2), which eventually ceased to exist and left an edge parallel to the face (11$\bar{2}$2).

4. Conclusion

The fact of occurrence of faceting of islands of semipolar GaN(11$\bar{2}$2) during epitaxy on substrates NP-Si(113) was established. The fact that a predominant growth of

the crystal faces of *m*-GaN in comparison with *c*-GaN is observed is due not only to the Gibbs–Curie–Wolfe selection principle during the formation of crystals under equilibrium conditions, but it is also attributable to the impact of elastic stresses in the plane of *c*-GaN and possibly different diffusion lengths of Ga atoms along and across the groove.

Acknowledgments

Conflict of interest

The authors declare that they have no conflict of interest.

References

[1] T. Wang. Semicond. Sci. Technol., **31**, 093003 (2016).

[2] D. Zhu, D.J. Wallis, C.J. Humphreys. Rep. Progr. Phys., **76**, 106501 (2013).

[3] A. Dadgar, J. Bläsing, A. Diez, A. Alam, M. Heuken, A. Krost. Jpn. J. Appl. Phys., **39**, L1183 (2000).

[4] H. Ibach, H.D. Bruchmann, H. Wagner. Appl. Phys. A, **29**, 113 (1982).

[5] M. Khoury, O. Tottereau, G. Feuillet, P. Vennégués, J. Zúñiga-Pérez. J. Appl. Phys., **122**, 105108 (2017).

[6] R. Mantach, P. Vennégués, J. Zuniga Perez, P. DeMierry, M. Leroux, M. Portail, G. Feuillet. J. Appl. Phys., **125**, 035703 (2019).

[7] N. Suzuki, T. Uchida, T. Tanikawa, T. Hikosaka, Y. Honda, M. Yamaguchi, N. Sawaki. J. Cryst. Growth, **311**, 2875 (2009).

[8] Y. Cai, X. Yu, S. Shen, X. Zhao, L. Jiu, C. Zhu, J. Bai, T. Wang. Semicond. Sci. Technol., **34**, 045012 (2019).

[9] H.-J. Lee, S.-Y. Bae, K. Lekhal, A. Tamura, T. Suzuki, M. Kushimoto, Y. Hond, H. Amano. J. Cryst. Growth, **468**, 547 (2016).

[10] H. Li, H. Zhang, J. Song, P. Li, Sh. Nakamura, S.P. DenBaars. Appl. Phys. Rev., **7**, 041318 (2020).

[11] J. Bruckbauer, C. Trager-Cowan, B. Hourahine, A. Winkelmann, Ph. Vennégués, A. Ipsen, X. Yu, X. Zhao, M.J. Wallace, P.R. Edwards, G. Naresh-Kumar, M. Hocker, S. Bauer, R. Mü ller, J. Bai, K. Thonke, T. Wang, R.W. Martin. J. Appl. Phys., **127**, 035705 (2020).

[12] V.N. Bessolov. E.V. Konenkova, S.N. Rodin, D.S. Kibalov, V.K. Smirnov. FTP, **55** (4),356 (2021). (in Russian).

[13] V.N. Bessolov, E.V. Konenkova, T.A. Orlova, S.N. Rodin, A.V. Solomnikova. ZhTF, **92** (5), 720 (2022). (in Russian).

[14] V.N. Bessolov, M.E. Kompan, E.V. Konenkova, S.N. Rodin. Izv. Ross. Akad. Nauk. Ser. Fiz., **86**(7), 981 (2022). (in Russian).

[15] K. Hiramatsu, K. Nishiyama, M. Onishi, H. Mizutani, M. Narukawa, A. Motogaito, H. Miyake, Y. Iyechika, T. Maeda. J. Cryst. Growth, **221**, 316 (2000).

[16] G. Feng, Y. Fu, J.S. Xia, J.J. Zhu, B.S. Zhang, X.M. Shen, D.G. Zhao, H. Yang, J.W. Liang. J. Phys. D, **35**, 2731 (2002).

[17] B.K. Weinstein, A.A.Chernov, L.A.Shuvalov. *Sovremennaya kristallografiya*. V. 3. *Obrazovanie kristallov* (M., Nauka, 1980) p. 408.

[18] I.Sunagawa. *Crystals Growth, Morphology, and Perfection* (Cambridge University Press, N.Y., USA, 2005).

[19] T. Akiyama, Y. Seta, K. Nakamura, T. Ito. Phys. Rev. Mater., **3**, 023401 (2019).

[20] M. Razia, M. Chugh, M. Ranganathan. Appl. Surf. Sci., **566**, 150627 (2021).

[21] K. Wang, R. Kirste, S. Mita, Sh. Washiyama, W. Mecouch, P. Reddy, R. Collazo, Z. Sitar. Appl. Phys. Lett., **120**, 032104 (2022).

[22] T.J. Baker, B.A. Haskell, F. Wu, P.T. Fini, J.S. Speck, S. Nakamura. Jpn. J. Appl. Phys., **44**, L920 (2005).

[23] C. Liu, S. Stepanov, P.A. Shields, A. Gott, W.N. Wang, E. Steimetz, J.-T. Zettler. Appl. Phys. Lett., **88**, 101103 (2006).

Translated by A.Akhtyamov